Proceedings of the 12th International Conference on
Aluminium Alloys, September 5-9, 2010, Yokohama, Japan

pp. 1746-1751

Characterization of Dendrite Morphology for Al-based Alloy by Phase-field Model

Yukinobu Natsume[1] and Hitoshi Ishida[1]
[1]Materials Research Laboratory, Kobe Steel, LTD,
1-5-5, Takatsukadai, Nishi-ku, Kobe, Hyogo, 651-2271, Japan

Numerical simulation of dendrite growth was carried out for Al-Si alloy by using a phase-field model, investigating dendrite morphology and secondary dendrite arm spacing. As the condition, we calculated between liquidus temperature for each alloy composition and eutectic temperature, and a planar initial solid was set on the bottom of calculated domain. Initial planer solid grew to be cellular morphology because of the perturbation on the solid-liquid interface, and then coarsening and competitive growth due to the growth of secondary arm occurred. Moreover, the morphologies were changed by alloy composition and cooling rate. As a result, the exponents for secondary arm spacing were in proportion to about -1/3 of cooling rate and about 1/3 of local solidification time, and these relationships were in good agreement with the experimental data and an analytical model. Therefore, we found the phase-field model is effective for quantitative simulations like the prediction for secondary dendrite arm spacing.

Keywords: *solidification, simulation, phase-field model, dendrite, secondary dendrite arm spacing*

1. Introduction

Nearly all of the solidification microstructures formed by a pure metal or an alloy casting were poly-crystal or poly-phase structures. The most basic and important growth form is the dendrite. The dendrite growth relates to some casting defects such as micro-segregation, cavity and porosity, that is, the complex growth patterns of dendrite remain as the micro-segregation and cavity or porosity forms between arms. Thus, the complex growth patterns of dendrite have been investigated experimentally and theoretically. Some theoretical models for the growth of dendrite tip have been developed, the Lipton-Kurz-Trivedi (LKT) model [1] is well known as the theoretical one described the dendrite tip growth at undercooling melt.

In casting products of aluminum alloy, the primary dendrite has a great influence on the mechanical property because the primary structure remains as the final one after solidification. Therefore, it is important to know how the primary dendrite formed as the microstructures, which are arm spacing, grain size and so on.

Recently, a phase-field model has been developed as the computational tool for a microstructure evolution [2-5]. The models of solidification for pure metal and an alloy have been developed rapidly since the simulation of the dendrite morphology was reported by Kobayashi [2], who simulated the dendrite morphology by considering the growth anisotropy in the model.

In the present work, we carried out phase-field simulations of dendrite growth for aluminum-silicon alloy, which is the basic aluminum alloy for casting, and investigated about the dendrite morphology and secondary arm spacing.

2. Phase-field Model

The phase-field model for a binary alloy is calculated by two governing equations, which are phase-field and diffusion equations. Equations (1) and (2) are for the phase-field and the diffusion of solute, respectively. Equation (3) is free energy density function including Eq. (1). The first term in Eq. (3) means a chemical free energy, which is given by Eq. (4), the second one means a double-well

potential energy and the third one means an interfacial gradient energy. Equation (5) is the concentration mixture rule with an interpolated function, $h(\phi)$.

$$\frac{\partial \phi}{\partial t} = -M \frac{\delta F}{\delta \phi} \tag{1}$$

$$\frac{\partial c}{\partial t} = \nabla \cdot \left(\frac{D}{f_{cc}} \nabla f_c \right) \tag{2}$$

$$F = \int_V \left(f(\phi, c, T) + Wg(\phi) + \frac{\varepsilon^2}{2} (\nabla \phi)^2 \right) dV \tag{3}$$

$$f(\phi, c, T) = h(\phi) f^S(c_S) + (1 - h(\phi)) f^L(c_L) \tag{4}$$

$$c = h(\phi) c_S + (1 - h(\phi)) c_L \tag{5}$$

where ϕ is a phase-field which is ϕ=0 in liquid and ϕ=1 in solid, c_S and c_L are concentrations of solute in solid and in liquid, respectively, and these values are determined by the condition of equal chemical potentials at each point, $f^S{}_{cS} = f^L{}_{cL}$. D is a diffusion coefficient, T is a temperature, f^S and f^L are free energy density in solid and in liquid, respectively. Interpolated functions are given by $g(\phi)=\phi^2(1-\phi)^2$ and $h(\phi)=\phi^2(3-2\phi)$. The subscripts c and cc under f denotes the partial derivative. M, ε and W are phase-field parameters which are very important parameters described quantitatively the dynamics of the S/L interface. The ε and W are related to an interfacial energy, σ, and an interfacial thickness, 2λ, as follows:

$$\sigma = \frac{\varepsilon \sqrt{2W}}{8} \pi \tag{6}$$

$$2\lambda = \frac{\varepsilon}{\sqrt{2W}} \pi \tag{7}$$

The M is a phase-field mobility given by the thin interface limit condition at KKS model [5].

$$\begin{aligned} M^{-1} &= \frac{\varepsilon^2}{\sigma} \left[\frac{RT}{V_m} \frac{1-k}{m} \beta + \frac{\varepsilon}{D\sqrt{2W}} f^S_{cc}(c^e_S) f^L_{cc}(c^e_L)(c^e_L - c^e_S)^2 \xi(\phi, c^e_S, c^e_L) \right] \\ \xi(\phi, c^e_S, c^e_L) &= \int_0^1 \frac{h(\phi_0)[1-h(\phi_0)]}{[1-h(\phi_0)] f^S_{cc}(c^e_S) + h(\phi_0) f^L_{cc}(c^e_L)} \frac{d\phi_0}{\sqrt{g(\phi_0)}} \end{aligned} \tag{8}$$

where R is the gas constant, V_m is a molar volume, k is a partition coefficient, m is a liquidus slope and β is a kinetic coefficient. The superscript e below c_S and c_L denote the equilibrium condition.

In order to simulate the dendrite morphology, the growth anisotropy has to be given for the interfacial energy or mobility. In the present model, the anisotropy for four fold symmetry is given in the interfacial gradient energy coefficient, ε, as follows:

$$\varepsilon = \varepsilon_0 (1 + \varepsilon_4 \cos 4\theta) \tag{9}$$

where ε_4 is a constant and $\theta = \tan^{-1}(\phi_y / \phi_x)$.

3. Calculation conditions

Equations (1) and (2) are solved by using a finite difference method. The calculation was carried out for Al-5, 7 and 9 mass% Si binary alloys. Table shows the material properties of aluminum-silicon binary alloy [6]. Calculation domain is two-dimensional as shown in Fig.1. We set the initial planar

solid on the bottom of the calculation domain and assumed it to be the primary dendrite arm. The size of calculation domain, 120 μm x 40 μm, was divided into square grids with 0.1 μm on the *x*- and *y*-coordinates. The right and left sides of calculation domain are the periodic boundary condition and the upper and lower sides are adiabatic boundary condition. The system temperature was uniform in the calculation domain and was changed from liquidus temperature, T^*, to eutectic temperature, T_e, as shown in Fig. 2. The cooling rates were used 10 to 200 K/s.

Table Material properties of Al-Si binary alloy used in the simulation.

Al-Si binary alloy	
Partition coefficient, k_0	0.13
Liquidus slope, m [K/mass%Si]	-6.00
Diffusivity in Solid, D_S [m^2/s]	1.0×10^{-12}
Diffusivity in Liquid, D_L [m^2/s]	3.0×10^{-9}
Molar volume of Al, $V_{m,Al}$ [m^3/mol]	1.00×10^{-5}
Molar volume of Si, $V_{m,Si}$ [m^3/mol]	1.21×10^{-5}
Interfacial energy, σ [J/m^2]	0.160
Anisotropy parameter, ε_4	0.03
Gibbs-Thomson coefficient, Γ	1.60×10^{-7}

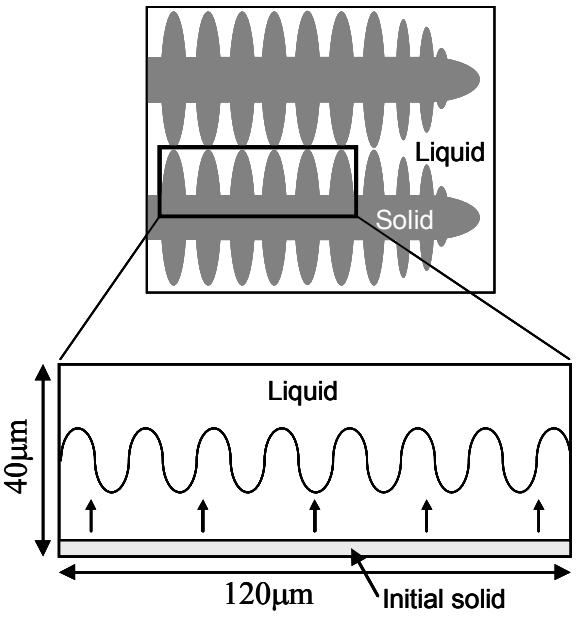

Fig.1 Schematic illustration of calculation domain used in the simulation.

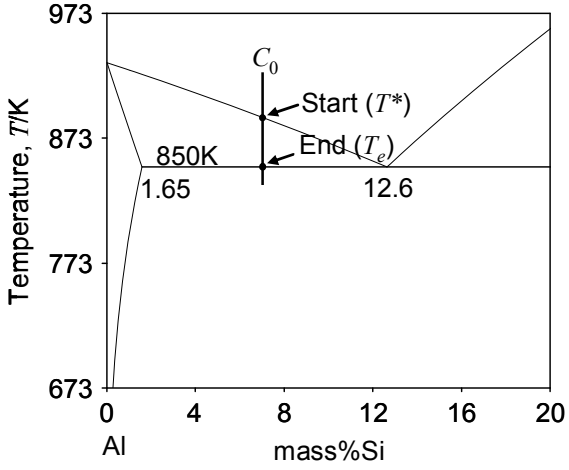

Fig.2 Phase diagram of Al-Si binary alloy system.

4. Results and discussion

4.1 Evolution of the dendrite morphology

Figure 3 shows the evolution of calculated silicon concentration profiles for Al-5mass%Si alloy at the cooling rate of 50 K/s. Initially, the planar S/L interface grew, and then became cell-like interface by the perturbation of the interface. The cells, regarded as the secondary dendrite arm, developed with the selection and coarsening of the arms. The small arms denoted by A (Arm-A) were melted and eliminated by the growth of their neighbors. In addition, in the arms denoted by B (Arm-B), the coalescence of two small arms occurred near the tips due to coarsening, and the liquid droplet between the arms formed.

Several mechanisms have been proposed to describe the coarsening [7-11]. The mechanism of coarsening for the Arm-A is similar to the model proposed by Reeves and Kattamis [8], and that for the Arm-B is similar to the model proposed by Mortensen [9].

Recently, Terzi *et al*. [11] have modeled the mechanisms of coarsening of Al-Cu alloy. Their models were developed by their experimental results based on *in-situ* observation by X-ray tomography, and they proposed three coarsening mechanisms, which are small arm melting (SAM), interdendritic groove advancement (IGA) and coalescence and groove advancement (CGA). The SAM is the coarsening mechanism that the small arm between bigger arms dissolves, the IGA is the one that the interdendritic space is filled by the movement of the base of the interdendritic liquid toward the tips, and the CGA is the one which involves coalescence of the dendrites near the tip, leading to entrapment of liquid in the solid. According to their mechanisms, the mechanism of the Arm-A corresponds to the SAM, and that of the Arm-B corresponds to the CGA. Moreover, the IGA occurs in liquid grooves between arms.

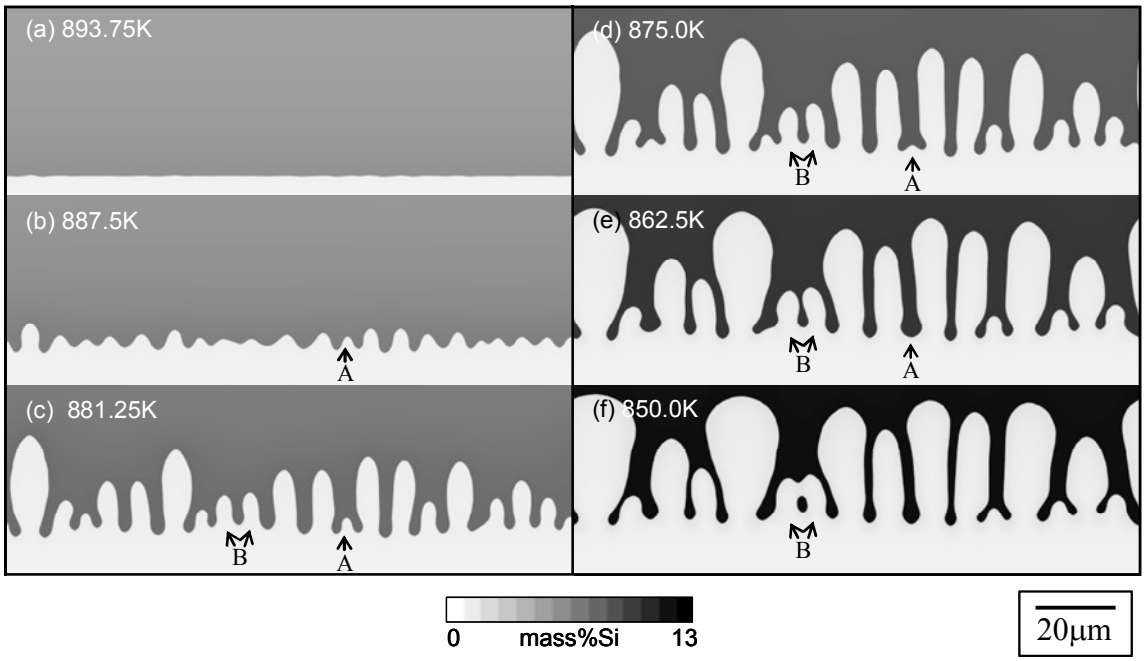

Fig.3 Evolution of calculated Si concentration profiles for Al-5mass%Si alloy simulated by phase-field method (50K/s).

4.2 Prediction of the secondary dendrite arm spacing

Figure 4 shows the relationship between cooling rate and secondary dendrite arm spacing (SDAS) for Al-Si binary alloy calculated by the phase-field model. We estimated the SDAS at eutectic temperature. The values of the SDAS decreased with an increase in cooling rate, and most values were linearly plotted. The slope of the line is -0.325, the exponent of the SDAS is in proportion to about -1/3 of cooling rate.

Figure 5 shows the relationship between local solidification time and the SDAS for Al-Si binary alloy calculated by the phase-field model. The experimental data reported by Okamoto *et al*. [12,13] are plotted for comparison. The broken line is the experimental data and the solid line is our simulated results. The SDAS increased with an increase in local solidification time, and the simulated results were good agreement with the experimental data. The slope of the line for our simulation is 0.326, the exponent of the SDAS is in proportion to about 1/3 of local solidification time.

A theoretical model of the coarsening predicts the relation that the SDAS, λ_2, is in proportion to the cube root of local solidification time, t_f. Following Kattamis *et al*. [14], one can write:

$$\lambda_2 = 5.5(At_f)^{1/3} \tag{10}$$

with

$$A = -\frac{\Gamma D_L \ln(C_L^m / C_0)}{m(1-k)(C_L^m - C_0)} \tag{11}$$

where Γ is Gibbs-Thomson coefficient and C_L^m is final liquid concentration, here C_L^m corresponds to the eutectic concentration. Calculating the coefficient, $5.5A^{1/3}$, in Eq. (10) for each alloy, the values of the coefficient at Al-5, 7 and 9 mass%Si alloys were 11.9, 11.3, and 10.9 μm/s$^{1/3}$, respectively. Similarly, calculating the coefficient from the simulated results, the values for each alloy were 9.93, 9.88 and 9.81 μm/s$^{1/3}$, respectively. Here, we assumed that the exponent of the SDAS is proportional to the 1/3 of local solidification time. The values obtained from the simulated results were in good agreement with those of theoretical model.

As the results, the results of our simulation were in good agreement with that of the experiment and the theoretical model. Thus, it was found that the phase-field model can quantitatively predict the SDAS.

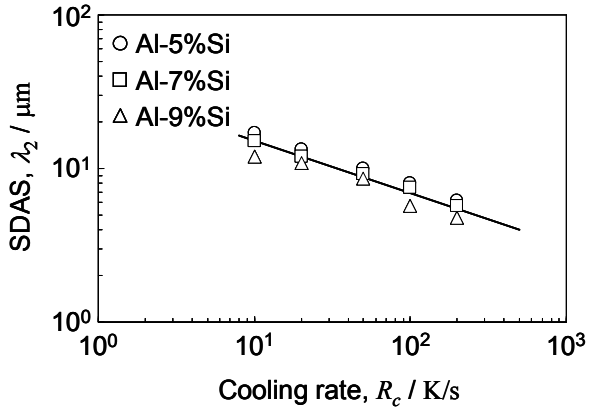

Fig.4 Relationship between cooling rate and secondary dendrite arm spacing at eutectic temperature for Al-Si binary alloy simulated by phase-field method.

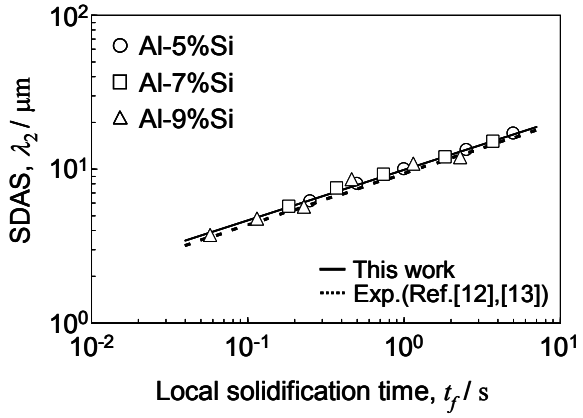

Fig.5 Relationship between local solidification time and secondary dendrite arm spacing at eutectic temperature for Al-Si binary alloy simulated by phase-field method.

5. Conclusions

We carried out numerical simulation of dendrite growth for Al-Si alloy by using the phase-field model. By investigating about the dendrite morphology and the SDAS, we evaluated the potential for quantitative prediction of the phase-field model.

(1) The dendrite coarsening can be simulated by the phase-field model, and three coarsening mechanisms, which are the SAM, CGA and IGA proposed by Terzi *et al.*, occurred in the simulated dendrite growth.

(2) The exponent of the SDAS of our simulation for Al-Si alloy was proportional to about -1/3 of cooling rate and about 1/3 of local solidification time. The relationships were in good agreement with the experimental results and the theoretical model.

References

[1] J. Lipton, W. Kurz and R. Trivedi: Acta Metall. 35 (1987) 957-964
[2] R. Kobayashi: Physica D, 63 (1993) 410-423
[3] A. Karma and W. -J. Rappel: Phys. Rev. E 57 (1998) 4323-4349
[4] A. A. Wheeler, W. J. Boettinger and G. B. McFadden: Phys. Rev. A 45 (1992) 7424-7439
[5] S. G. Kim, W. T. Kim and T. Suzuki: Phys. Rev. E, 60 (1999) 7186-7197

[6] W. Kurz and D. J. Fisher: *Fundamentals of solidification*, 4th Ed. (Trans Tech Publications, Switzerland, 1998) pp. 293-294
[7] T. Z. Kattamis, J. C. Coughlin and M. C. Flemings: Trans AIME 239 (1967) 1504-1511
[8] J. J. Reeves and T. Z. Kattamis: Scripta Metall. 5 (1971) 223-227
[9] A. Mortensen: Metall Trans A 20A (1989) 247-253
[10] M. Chen and T. Z. Kattamis: Mater. Sci. Eng. A 247 (1998) 239-247
[11] S. Terzi, L. Salvo, M. Suery, A. K. Dahle and E. Boller: Acta Mater. 58 (2010) 20-30
[12] T. Okamoto and K. Kishitake: J. Crystal Growth 29 (1975) 137-146
[13] T. Okamoto: Bull. Jap. Institute of Metals 17 (1978) 731-738
[14] T. Z. Kattamis and M. C. Flemings: Trans. Metall. Soc. AIME 233 (1965) 992-999